Journal of Chemical Neuroanatomy 121 (2022) 102082

Contents lists available at ScienceDirect

Journal of Chemical Neuroanatomy

journal homepage: www.elsevier.com/locate/jchemneu

Nerve fiber density differences in the temporal dura mater: An explanation for headache after temporal lobectomy? An anatomical study

Jiske C.T. Sloekers [a,*], Andreas Herrler [b], Govert Hoogland [a,c,d], Kim Rijkers [a,c,d], Jan Beckervordersandforth [e], Sander M.J. van Kuijk [f], Olaf E.M.G. Schijns [a,c,d]

[a] Department of Neurosurgery, Maastricht University Medical Centre+, Maastricht, The Netherlands
[b] Department of Anatomy & Embryology, Maastricht University, Maastricht, The Netherlands
[c] School for Mental Health and Neuroscience (MHeNS), University Maastricht, Maastricht, The Netherlands
[d] Academic Center for Epileptology, Maastricht University Medical Centre+, Maastricht, The Netherlands
[e] Department of Pathology, Maastricht University Medical Centre+, Maastricht, The Netherlands
[f] Clinical Epidemiology and Medical Technology Assessment, Maastricht University Medical Centre+, Maastricht, The Netherlands

ARTICLE INFO

Keywords:
Headache
Temporal lobectomy
Epilepsy surgery
Nerve fiber density

ABSTRACT

Objective: Patients who undergo a temporal lobectomy for drug-resistant epilepsy more frequently complain about postoperative headache compared to patients who undergo a craniotomy in any other region. The pathophysiological mechanism is not well understood. It is hypothesized that a relatively high density of sensory nerve fibers in the temporomesial dura underlies a higher sensitivity to pain upon stimulation. The objective of this study was to address this hypothesis by comparing the nerve fiber density in the temporomesial dura to that in the temporolateral dura.

Methods: Temporomesial (n = 6) and temporolateral (n = 6) dura mater samples (2.5 × 2 cm) were dissected from the middle cranial fossa of 5 formalin fixed human cadavers. Paraffin embedded specimens were cut in a sagittal direction into 5 μm sections (temporomesial group n = 106, temporolateral group n = 113), and immunohistochemically stained for S100 as a marker of myelinated nerve fibers. The number of S100-immunoreactive nerve fiber bundles was counted in an anterior-posterior direction by a blinded observer, expressed as mean ± standard error of the mean per cm for each group, and statistically analyzed by a linear mixed-effects model. To assess potential observer bias, a randomized subset of the sections (n = 28) was evaluated by a second blinded observer and statistically analyzed by intraclass correlation coefficient (ICC).

Results: The temporomesial dura expressed 4.1 ± 2.1 and the temporolateral dura displayed 1.0 ± 0.7 nerve fiber bundles per cm ($\beta = 3.2$, SE= 0.30, 95% CI [2.6, 3.8], $p < 0.001$). There is a significant decrease in nerve fiber bundle density in the mesial to lateral direction (mean difference −0.1, SE= 0.0, 95% CI [−0.1, −0.2], $p < 0.001$). The ICC was 0.69.

Conclusions: The density of myelinated nerve fiber bundles is about 4 times higher in the temporomesial dura, than in the temporolateral dura. Assuming that dural innervation primarily consists of sensory trigeminal fibers, this observation suggests that a summation of stimuli to surpass the threshold to convey pain is reached sooner in the temporomesial than in the temporolateral dura mater.

1. Introduction

New-onset post-craniotomy headache is a common type of secondary headache, occurring within seven days after surgery (Headache Classification Committee of the International Headache, S (2013)). The reported incidence of new-onset headache after craniotomies in general is 40%, and is mainly related to the site of the surgical scar. Within three months, 10.7% of headaches are resolved, whereas 29.3% persists after three months (Rocha-Filho et al., 2008). Epilepsy surgery is an established, curative treatment option for patients with drug-resistant chronic epilepsy (Engel et al., 2012; Wiebe et al., 2001). The most frequently carried out type of epilepsy surgery in adults is temporal lobectomy with or without amygdalohippocampectomy. Afterwards, patients complain about a pain located deep inside the head. The reported associated risk of chronic post-craniotomy headache after temporal lobectomy for

* Correspondence to: Maastricht University Medical Centre+, Department of Neurosurgery, PO box 5800, 6202 AZ Maastricht, The Netherlands.
E-mail address: jiske.sloekers@mumc.nl (J.C.T. Sloekers).

https://doi.org/10.1016/j.jchemneu.2022.102082
Received 22 August 2021; Received in revised form 10 February 2022; Accepted 10 February 2022
Available online 11 February 2022
0891-0618/© 2022 The Authors. Published by Elsevier B.V. This is an open access article under the CC BY license (http://creativecommons.org/licenses/by/4.0/).

Nomenclature

CI	Confidence interval
ICC	Intraclass correlation coefficient
PBS	Phosphate buffered saline
V1	Ophthalmic branch of trigeminal nerve
V2	Maxillary branch of trigeminal nerve
V3	Mandibular branch of trigeminal nerve

epilepsy patients, whereby headaches deep inside the head persist for more than 1 year, and the majority even needs analgetic drugs or reports to experience medically uncontrollable headache, is 11.9% (Kaur et al., 2000). These findings combined, indicate that the experienced new-onset post-craniotomy headache is not simply pain of the wound.

Current treatment of new-onset post-craniotomy headache is based on symptom control, whereby various systemic (mostly opioids and acetaminophen) and local treatments (scalp infiltration) have been compared (Guilfoyle et al., 2013; Lutman et al., 2018; Molnar et al., 2014). Scalp infiltration, applied pre- and postoperatively, reduces direct postoperative pain on the visual analog scale (VAS) for 1–12 h postoperatively (Biswas & Bithal, 2003; Bloomfield et al., 1998; Guilfoyle et al., 2013), but does not lead to significant permanent headache reduction (Zhou et al., 2016), which is consistent with the fact that patients complain about a pain located deep inside the head. Most theories on its pathophysiology are based on manipulation of the dura, injury to cranial nerves and/or nerve entrapment, and/or central sensitization (Lutman et al., 2018; Molnar et al., 2014; Rocha-Filho, 2015). During a temporal lobectomy, the anterior part of the lateral and/or mesial temporal lobe is removed by suction, coagulation, and aspiration. Tissue is aspirated down to the skull base of the middle cranial fossa, whereby the overlying dura mater is frequently touched by micromanipulation with different surgical instruments. Lv et al. (2014) describe that the excitability of neurons in the intracranial dura mater can be increased by 'punctuate probing, stroking or traction', potentially contributing to the relatively high incidence of new-onset post-craniotomy headache after temporal lobectomy.

Intracranial dural innervation is provided by afferent fibers from the ophthalmic (V1), maxillary (V2) and mandibular (V3) branches of the trigeminal nerve, as well as by the sensory fascicles of the upper three cervical spinal nerve roots, and sympathetic fibers from several upper cervical ganglia and the sympathetic trunk (Andres et al., 1987; Bauer et al., 2005; Kemp et al., 2012; Lee, Hwang, et al., 2017; Lee, Shin, et al., 2017). The dural innervation can roughly be subdivided into the following main anatomical regions: the anterior, middle and posterior cranial fossae, the falx cerebri, the tentorium and the dura overlying the temporal, parietal, occipital and frontal regions of the skull convexity. Three major dural nerves have first been identified in rats, and later in humans: the anterior ethmoidal (V1), spinosus (V3) and tentorial (V1) nerves, all arising from trigeminal branches (Andres et al., 1987; Bauer et al., 2005).

The dura mater overlying the middle cranial fossa is innervated by the nervus spinosus and the middle meningeal nerve arising from V2. The nervus spinosus has been described recently (Lee, Hwang, et al., 2017; Schueler et al., 2014), and earlier in relation to headache by Penfield and McNaughton (1940) and Steiger et al. (1982). It re-enters the cranium through the foramen spinosum together with and parallel to the middle meningeal artery. It mainly innervates the posterior and lateral part of dura mater overlying the middle cranial fossa, whereby it does not enter the anterior cranial fossa, terminating before reaching the sphenoparietal sinus (Bauer et al., 2005; Kemp et al., 2012; Lee, Hwang, et al., 2017; Lee, Shin, et al., 2017; Penfield & McNaughton, 1940; Steiger et al., 1982). The middle meningeal nerve also runs parallel to the middle meningeal artery and mainly innervates the anterior dura of the middle cranial fossa and the dura over the lesser wing of the sphenoid bone (Bauer et al., 2005; Kemp et al., 2012; Lee, Shin, et al., 2017; Penfield & McNaughton, 1940; Steiger et al., 1982).

Detailed knowledge on nerve fiber density in different dural regions is lacking, yet here we hypothesize that the temporomesial dura mater in the middle cranial fossa contains more myelinated nerve fibers compared to the temporolateral dura. Surgical micromanipulation of this richly innervated dura can be an etiological factor explaining the high incidence of new onset headache after temporal lobectomy. The objective of this study was to quantify the density of myelinated nerve fibers in the human temporomesial and temporolateral dura of the middle cranial fossa.

2. Materials and methods

2.1. Subjects

Six specimens of dura mater were obtained from five human cadavers (female n = 3) provided by the Department of Anatomy and Embryology, Maastricht University, Maastricht, The Netherlands. Donors gave informed consent to donate their body for teaching and research purposes, according to the Dutch law for the use of human remains for scientific research and education ("*Wet op lijkbezorging*" BWBR0005009*)*. A handwritten and signed codicil from the donor is archived at the Department of Anatomy and Embryology.

Human cadavers, fixed in 10% phosphate buffered formalin, were stored at 4 °C. Prior to dissections the cadavers were washed for at least one hour in running tap water. The dura mater overlying the middle cranial fossa, including dura mater attached to the foramina rotundum, ovale and spinosum, was carefully dissected from the skull base. Both full pars meningealis and pars periostalis were preserved. One temporomesial and one lateral block of dura mater (minimally 2.5 ×2 cm) was cut out and both were sized to fit in an embedding cassette. The temporomesial block was cut out as a rectangle with the medial border measured through the foramina rotundum, ovale and spinosum, and the lateral border at least 2 cm more lateral to the mesial border. The temporolateral block was cut out as a rectangle measured from the far lateral side of the entire cut out dura mater specimen, with the medial border at least 2 cm more medial from the far lateral side (Fig. 1). Markings were attached to identify the posterior-lateral corner of both the mesial and lateral blocks. Thereafter, blocks were processed and embedded in paraffin, after which sagittal histological sections were cut using a microtome (Leica, RM2245). Every 1000 μm, a 5 μm section was cut and mounted on a polysine coated glass slide (n = 17–20). Sections were dried in an oven at 40 °C overnight and at 70 °C for at least an

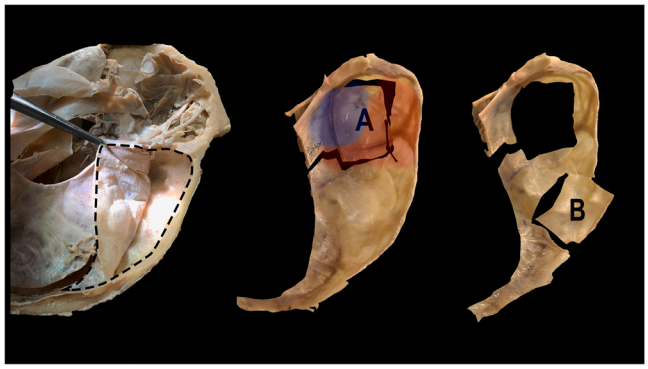

Fig. 1. Sampling of human dura mater. Left: the intact dura overlying and partly lifted from the middle cranial fossa, with a dashed line indicating the dissected part. Middle: temporomesial sampling (A), with blue indicating the innervation region of the middle meningeal nerve and red indicating the innervation region of the nervus spinosus. Right: temporolateral sampling (B). See methods section for landmark criteria.

additional hour before staining.

2.2. Immunohistochemistry

To identify all myelinated nerve fibers, sections were immunohistochemically stained for S100 at room temperature. S100 belongs to the family of calcium binding proteins. The antibody to S100 stains, among others, neurons and myelinated nerve fibers, Schwann cells and other glial cells. From each of the six dura mater specimens, 34–40 sections were stained (temporomesial (n = 17–20) and temporolateral (n = 17–20)). First, sections were deparaffinized with xylene for 5 min twice. Endogenous peroxidase was blocked for 10 min with 3% hydrogen peroxide (H_2O_2) in methanol. Then, sections were rehydrated by incubations in a gradient of ethanol from 100% to 50%, and washed in 0.1 M phosphate buffered saline (PBS). Next, sections were incubated 30 min in Teng-T (10 mM Tris, 5 mM EDTA, 0.15 M NaCl, 0.25% gelatin, 0.05% Tween 20) with 10% normal goat serum (NGS; Gibco, 16210–072) to block nonspecific binding of antibodies, 60 min with S100 (anti-S100, DAKO, Z0311; 1:1000 diluted in Teng-T with 10% normal goat serum), and then 30 min with biotinylated goat anti-rabbit IgG (Vector, BA1000; 1:500 diluted in PBS with 0.1% Tween-20) as secondary antibody. Finally, horseradish peroxidase-coupled avidin-biotin complex enhancement (HRP-ABC; Vector, PK6100) was applied for 30 min, followed by 3,3′-diaminobenzidine (DAB; Sigma Aldrich, D5905) chromogen staining. Between all steps, sections were washed 3 times for 5 min in PBS with 0.1% Tween-20. Finally, sections were dehydrated by incubation in a gradient of ethanol from 50% to 100%, then incubated in xylene and mounted with Entallan (MERCK) and cover slip. Positive controls were made with paraffin embedded sections of human ileum (5 μm sections), of which the nervous plexus is known to stain positive for S100 (Gfroerer et al., 2010). Negative controls consisted of dura sections that were submitted to the same staining procedure, without the primary antibody S100. Staining was done in batches of 40 sections (20 temporomesial and 20 temporolateral) and a positive and negative control were included in every batch.

2.3. Analysis

Section labels were covered, mixed and re-numbered to enable randomized and blinded analysis. Using MBF Bioscience Stereo Investigator software (version 11.03.1, MicroBrightField Inc.) with an Olympus (Olympus, BX51) microscope at 10x enlargement, equipped with an LEP 3″x2″ stepper motorized stage (Ludl Electronic Products, SS9000) and an MBF Bioscience digital camera (MicroBrightField Inc., CX9000), length of the dura mater was traced and nerve fiber bundles were marked and counted in all sections. Dura mater length was traced at the side of the inner dural blade lining the arachnoid, as this side consistently showed to be most continuous in the sections. A nerve fiber bundle was marked as such, when at least 3 positive stained cross-sectioned fibers were visible, located adjacent in a group together at 10x enlargement. A nerve fiber bundle was marked by this definition to prevent counting false positive staining as nerve bundles. When nerve fiber bundles were sectioned lengthwise, they were marked as one bundle. When a lengthwise bundle was sectioned multiple times, with a continuous dividing strip of connective tissue in between, they were marked as multiple bundles (Fig. 2). When a large bundle consisted of multiple sections, with a continuous dividing strip of connective tissue in between, each section was counted as one bundle. Density was calculated as nerve fiber bundles per cm dura mater length to enable quantitative analysis. Finally, nerve fiber bundle densities were averaged per quartile in both anterior-posterior and mesial-lateral direction per section, translating into an overview of the distribution of nerve fiber bundle density over the studied sections for both the temporomesial and -lateral blocks in all six dura specimens. A second blinded observer evaluated 28 randomized sections to assess inter-observer reliability.

2.4. Statistical analysis

Statistical analysis was performed in SPSS Statistics (version 25.0, IBM Corp, New York). Characteristics of the sections were described as mean and standard error of the mean (SEM). A linear mixed-effects model was used to assess the association between location of temporal dura mater (mesial vs lateral) and the density of nerve fiber bundles per cm. The linear-mixed effects model is a linear regression that takes the clustering of data within study subjects into account. Study subject and section number were added to the model, whereby section number enabled the analysis of gradient in nerve fiber bundle density over the mesial-lateral direction within sampled sections from both the lateral and the mesial temporal dura mater. Results were described as mean difference with 95% confidence interval (CI). Differences were considered statistically significant at $p < 0.05$. Furthermore, an inter-observer reliability assessment was performed using a two-way random, consistency, single-measures intraclass correlation coefficient (ICC).

3. Results

A total of 219 sections was used for analysis (temporomesial (n = 106) and temporolateral (n = 113). All values were normally distributed. The average anterior-posterior-length of all temporomesial sections was 28.2 mm (SE= 0.4) and of all temporolateral sections 28.4 mm (SE=0.3). As visualized in overview Fig. 3, the nerve bundle densities in the medial, anterior and posterior regions were higher than those observed in the lateral and central regions within the temporomesial dura. In contrast, an overall lower and more equal distribution was observed in the subregions of the temporolateral region.

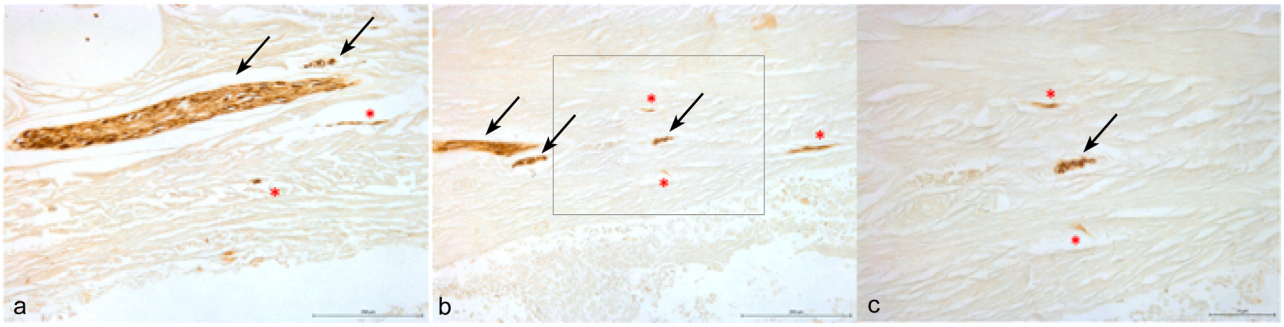

Fig. 2. Photomicrographs of S100-immunoreactive nerve fiber bundles in the temporomesial dura mater. Fiber bundles presented as lengthwise sectioned and surrounded by connective tissue. An arrow marks an individual counted nerve fiber bundle, a red asterisk marks positive stainings that were not counted as a nerve fiber bundle. Photomicrographs a and b in magnification x 10, with the scalebar indicating 250 μm. Photograph c representing the square box in photograph b, in magnification x 20, with the scalebar indicating 75 μm.

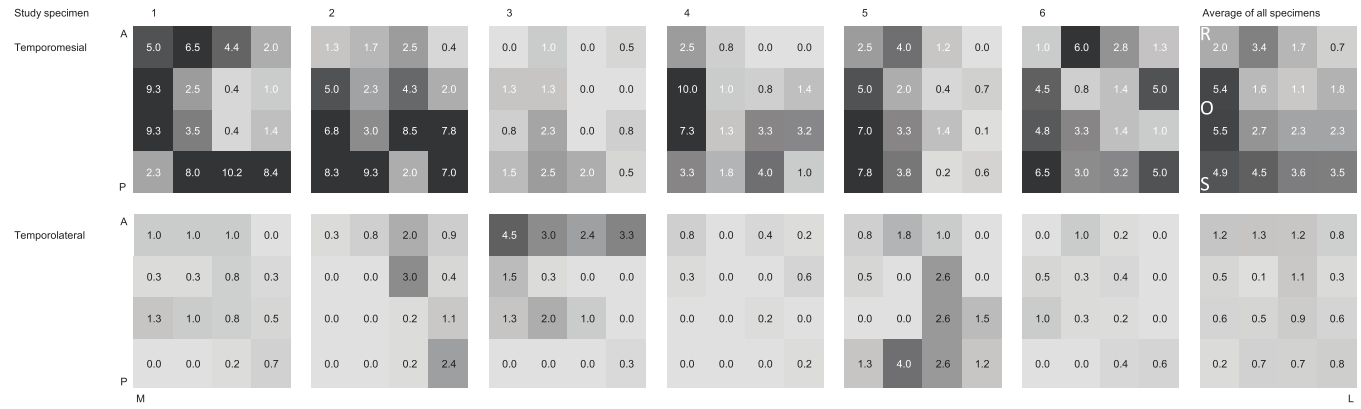

Fig. 3. Overview with numerical averages of the estimated distribution of mean nerve fiber bundle density throughout the temporomesial and temporolateral blocks of dura mater studied of the 6 specimens. Mean values for the nerve fiber bundle density for each quartile are depicted in the anterior (A) to posterior (P) and mesial (M) to lateral (L) direction, and written inside. Averages of all specimens were calculated not by averaging all averages in above displayed overviews, but by averaging all raw nerve bundle counts. Foramen rotundum (R), foramen ovale (O) and foramen spinosum (S) are indicated in the averaged overview.

The mean nerve fiber bundle density for the temporomesial location was 4.1 (SE= 2.1) bundles/cm and for the temporolateral location 1.0 (SE= 0.7) bundles/cm (Fig. 4; mean difference 3.2, SE= 0.3, 95% CI [2.6, 3.8], $p < 0.001$). This difference stayed highly significant when we analyzed the association between section number and nerve fiber bundle density in either the lateral or mesial location (mean difference −0.1, SE= 0.0, 95% CI [−0.1, −0.2], $p < 0.001$), indicating that there is a significant decrease in nerve fiber bundle density over all sections from one location in the mesial to lateral direction (Fig. 5). This effect remained significant if the product of study subject and section number was added to the model (mean difference −0.3, SE= 0.0, 95% CI [−0.2, −0.4, $p < 0.001$), indicating there is also an interaction between nerve fiber bundle density and section number within all study subjects separately. Results are summarized in Table 1. Inter-observer reliability was good, according to Cicchetti's interpretation of an ICC between 0.60 and 0.75 as good, with an ICC of 0.69 (Cicchetti, 1994).

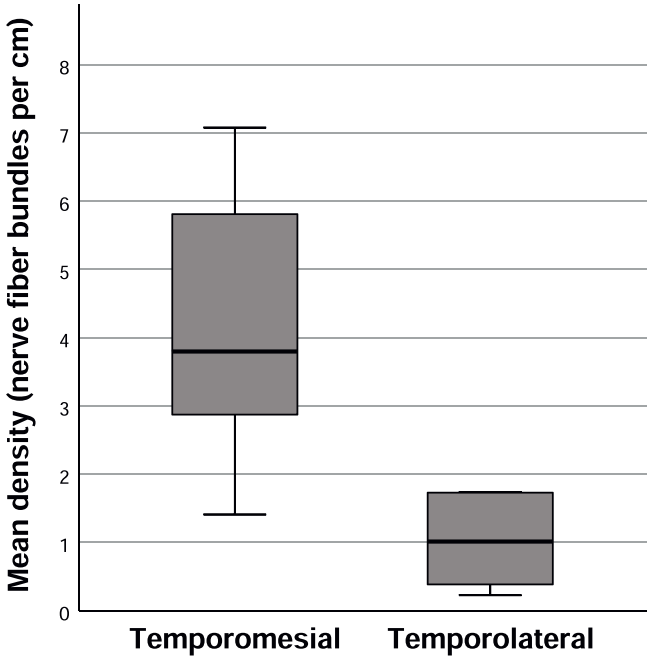

Fig. 4. Distribution of nerve fiber bundle densities in the temporomesial (n = 106) and temporolateral (n = 113) dura samples.

4. Discussion

A moderate to high incidence of new-onset post-craniotomy headache after temporal lobectomy for drug-resistant epilepsy is frequently reported. The pathophysiological mechanism for new-onset post-craniotomy headache is not well understood, although a possible explanation consists of an increased excitability of nociceptive myelinated nerve fibers by surgical manipulation of the dura mater (Lutman et al., 2018; Lv et al., 2014; Molnar et al., 2014; Rocha-Filho, 2015).

Our study demonstrated that the nerve fiber density of the dura mater is statistically significantly higher in the temporomesial region than in the lateral region (Fig. 3), which supports the possible explanation abovementioned.

The overview images with numerical averages portray the clear difference in nerve fiber density between the two regions. This appears to correspond to the location of two major sensory nerves innervating the dura mater of the middle cranial fossa: the nervus spinosus (V_3), and the middle meningeal nerve. The nervus spinosus enters the dura mater through the foramen spinosum (Penfield & McNaughton, 1940; Steiger et al., 1982), while the middle meningeal nerve originates from the maxillary nerve (V_2) in proximity of the foramen rotundum (Kemp et al., 2012; Penfield & McNaughton, 1940). The dense segments medially in the overview (Fig. 3) correspond with the points of origin of these two nerves: the anterior dense segment corresponds with the middle meningeal nerve whereas the posterior dense segment corresponds with the nervus spinosus, respectively (Kemp et al., 2012; Lee, Hwang, et al., 2017; Schueler et al., 2014).

After its entry into the dura mater, the nervus spinosus aims towards the sphenoparietal sinus, innervating the middle cranial fossa oriented anteriorly in the direction of the pterion. This has been demonstrated by Lee, Hwang, et al. (2017) and Penfield and McNaughton (1940), who have both described that the nervus spinosus terminates before reaching the sphenoparietal sinus. Since the middle meningeal nerve is located anteriorly of the nervus spinosus, there is no innervation in the middle cranial fossa posterior of the nervus spinosus. The innervation of dura mater of the more posteriorly located tentorium cerebelli is supplied by the tentorial nerve (V_1). Only rarely it crosses the transverse sinus to supply the lateral convexity (Lee, Shin, et al., 2017). So, since the nervus spinosus aims anteriorly and the tentorial nerve posteriorly, it can be deduced that the region in between, the temporolateral region aiming towards the lateral convexity, is only sparsely innervated. In a study focusing on catecholaminergic fibers in the dura mater, Cavallotti et al. (1998) concluded that innervation of the dura mater covering the skull base is more dense than the dura mater covering the skull convexity. However, because the dura mater is not only innervated by catecholaminergic fibers (Lv et al., 2014), the added value of our study is the

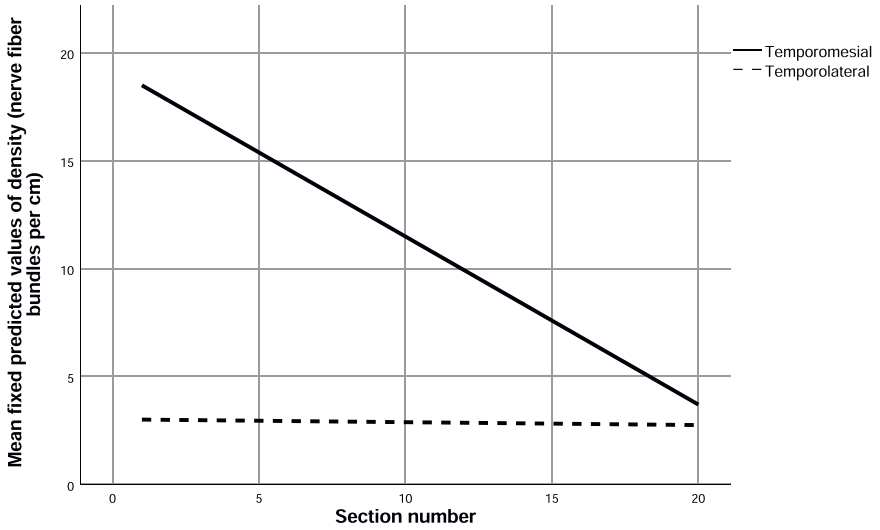

Fig. 5. Multiple line mean of fixed predicted values by section number and location of dura mater, depicting a significant negative linear relationship between nerve fiber bundle density and mesial to lateral distance over the sampled sections per location ($p < 0.001$).

Table 1
Estimate effects of the linear mixed model analysis. Model 1 shows a mean difference of 3.2 bundles/cm between the temporomesial and temporolateral dura mater. Model 2 shows a decline of 0.1 bundles/cm from the medial to lateral side of the temporomesial and temporolateral dura mater, indicating a difference in density from the medial to lateral side of the dura mater cutouts. And model 3 indicates that this decline is significant within each study subject separately.

Parameter	Model 1			Model 2			Model 3		
	Mean difference (SE)	95% CI	P	Mean difference (SE)	95% CI	P	Mean difference (SE)	95% CI	P
Location dura mater	3.2 (0.3)	2.6 – 3.8	< 0.001	3.1 (0.3)	2.6 – 3.7	< 0.001	5.7 (0.6)	4.7 – 6.8	< 0.001
Section number				-0.1 (0.0)	-0.2–0.1	< 0.001	-0.6 (0.1)	-0.4 to – 0.7	< 0.001
Section number per person							-0.3 (0.0)	-0.2 to – 0.4	< 0.001

staining and quantification of all myelinated nerve fibers in the temporomesial and lateral region, which to our knowledge has not been performed so far. Our study delivered evidence that the temporolateral region, towards the lateral skull convexity, is much more sparsely innervated than the temporomesial dura mater overlying the skull base of the middle cranial fossa.

In animal (rat and cat) studies it has been demonstrated that most nerve fibers in the cranial dura mater branch away from their primary myelinated nerve of origin and end as free unmyelinated nerve terminals in the connective tissue of the dura mater (Messlinger et al., 1993; Strassman et al., 2004). Therefore, presumably, a higher density in nerve fiber bundles in the temporomesial region of dura mater subsequently indicates a higher density in free unmyelinated nerve endings. Previous studies have shown that the density of nerve fibers in dermal tissue correlates with the sensory function of the skin, whereby a higher intra-epidermal nerve fiber density results in a better detection of stimuli and a better tactual acuity (Johansson & Vallbo, 1979; Mouraux et al., 2012). A lower intra-epidermal nerve fiber density resulted in higher pain thresholds (Schley et al., 2012). Therefore, a higher density in free nerve endings in the connective tissue would presumably lead to a higher nociceptive potentiality. However, this has not been confirmed with clinical data from studies with dural tissue. It is in line with a recent observational study regarding awake craniotomies by Fontaine et al. (2018), who concluded that the mesial dura mater overlying the skull base of the middle cranial fossa and the dura of the falx cerebri are quite sensitive to mechanical stimuli, provoking pain. A similar observation, with patients undergoing awake craniotomy for epilepsy and tumors in the temporal lobe, has been made in our center. Intraoperative feedback from our patients indicates that they experience an intense pain as soon as we touch the temporo-basal dura on the skull base, which decreases once the dura is no longer touched. Previous research also confirmed that stimulation or surgical manipulation of especially the skull base dura mater evokes pain (Fontaine & Almairac, 2017; Fontaine et al., 2018; Ray & Wolff, 1940). During a resection of the amygdala-hippocampal complex in the temporo-mesial region, the skull base dura mater of the middle cranial fossa will be manipulated by suction and coagulation, which intrinsically belongs to this type of surgery. The lateral convexity dura will be touched upon only sparsely. Therefore, as the temporo-lateral dura is continuous with the extra-temporal convexity dura and we rarely encounter these headache complaints in patients surgically treated in extratemporal regions, we do believe the crux of the difference is the inclusion or not of the temporo-mesial dura in the surgical procedure. Studies specifically comparing these two approaches do, to our knowledge, not exist in current neurosurgical literature.

Mechanosensitive neural receptors in the dura mater can be activated by local stroking or traction, as performed during microsurgical procedures with dural coagulation and manipulation by bipolar forceps or suction tubes (Lv et al., 2014). These mechanically insensitive afferents in the connective tissue of the dura mater may become mechanically sensitive and play a role as a nociceptive source in inflamed tissues (Lv et al., 2014; Messlinger et al., 1993). In the introduction we describe that injury to nerves and/or nerve entrapment, and/or central sensitization are the mechanisms on which theories for long lasting post craniotomy headache are based (Lutman et al., 2018; Molnar et al., 2014; Rocha-Filho, 2015). There is, most probable, more than one factor leading to central sensitization. Some are predisposing factors like pre-existing pain thresholds, partly due to multiple genetic factors (Phillips & Clauw, 2011), or psychophysiological factors like the stress-response. There is direct experimental evidence on humans showing a relationship between stress and lowering of pain thresholds (Rivat et al., 2010). It can be assumed that dural manipulation with local stroking and traction may cause the abovementioned damage and mechanisms leading to long lasting post craniotomy headache. As far as

we know, there is currently no literature regarding the correlation between post craniotomy headache and surgery outcomes like seizure freedom. Ives-Deliperi and Butler (2017) describe that quality of life improves significantly after epilepsy surgery, together with a reduction in depressive symptoms. However, they describe that quality of life was not significantly related to seizure freedom after epilepsy surgery and, as we mentioned above, the relation of headache to these outcomes has not been described.

Finally, the majority of myelinated axons have a sensory function (Strassman et al., 2004), and combined with our novel finding of a higher density of myelinated nerve fiber bundles in the temporomesial dura mater, this supports the presumption of a higher nociceptive potentiality of the temporomesial skull base dura compared to the lateral dura of the convexity.

To summarize, repeated surgical micromanipulation of the mechanosensitive neural receptors in the temporomesial dura mater delivers a probable pathophysiological mechanistic explanation for, and which via the concept of central sensitization can be cause and effect of, new-onset post-craniotomy headache after temporal lobectomy.

4.1. Limitations and recommendations for further research

The main limitation of our study is that we did not quantify the density of unmyelinated nerve fibers and free nerve endings in the dural connective tissue. Therefore, further studies could be designed with fluorescent immunohistochemistry. Either neurofilament protein or protein gene product 9.5 may be used as neuronal marker for unmyelinated nerve fibers, whereby as little variation in staining intensity as possible should be aimed for. Subsequently, optical densimetry and randomized computerized counting methods can be applied to quantitatively analyze the density of unmyelinated nerve fibers. Another limitation is that we have no clinical data to corroborate our laboratory findings. We do have a large personal experience based on surgeries performed in our center, which we have described in the discussion above. It is our intention to prepare a clinical study comparing temporolateral versus temporo-mesial dura mater manipulation in temporal versus extratemporal lobe surgery.

5. Conclusion

This study is the first, to our knowledge, that quantified densities of myelinated nerve fiber bundles in the temporomesial and temporolateral region of the human dura mater overlying the middle cranial fossa. In addition to a different expression between these two regions, we also observed a decreased nerve fiber bundle density from mesial to lateral direction in each section, which remained significant when analyzed within each study subject separately. Assuming the dural innervation primarily consists of sensory afferent trigeminal nerve fibers, the assumption can be made that the temporomesial dura mater is more pain sensitive than the temporolateral dura mater. Surgical micromanipulation of the temporomesial dura during temporal lobectomy for drug-resistant epilepsy can contribute to the moderate to high incidence of new-onset post-craniotomy headache after temporal lobe surgery and should be avoided as much as possible.

Funding statement

This research received no specific grant from any funding agency in the public, commercial, or non-profit sector.

CRediT authorship contribution statement

Jiske C.T. Sloekers: Conceptualization, Data curation, Formal analysis, Writing – original draft, Writing – review & editing. **Andreas Herrler:** Conceptualization, Methodology, Supervision, Writing – review & editing. **Govert Hoogland:** Conceptualization, Methodology, Supervision, Writing – review & editing. **Kim Rijkers:** Methodology, Supervision, Writing – review & editing. **Jan Beckervordersandforth:** Formal analysis, Writing – review & editing. **Sander M.J. van Kuijk:** Formal analysis, Methodology, Writing – review & editing. **Olaf E.M.G. Schijns:** Conceptualization, Methodology, Supervision, Writing – review & editing.

Acknowledgment

We would gratefully like to thank P. van Dijk for his advising and assisting with histological staining and analyses, I. van Weersch for her work as second observer of the histological stainings and re-analyzing 28 sections, and H. Steinbusch for her advice regarding the analysis of histochemical stainings.

Conflict of Interest Statement

We report no conflict of interest concerning the materials and methods used in this study or the findings specified in this paper.

References

Andres, K.H., von During, M., Muszynski, K., Schmidt, R.F., 1987. Nerve fibres and their terminals of the dura mater encephali of the rat. Anat. Embryol. 175 (3), 289–301.

Bauer, D.F., Youkilis, A., Schenck, C., Turner, C.R., Thompson, B.G., 2005. The falcine trigeminocardiac reflex: case report and review of the literature. Surg. Neurol 63 (2), 143–148. https://doi.org/10.1016/j.surneu.2004.03.022.

Biswas, B.K., Bithal, P.K., 2003. Preincision 0.25% bupivacaine scalp infiltration and postcraniotomy pain: a randomized double-blind, placebo-controlled study. J. Neurosurg. Anesthesiol. 15 (3), 234–239.

Bloomfield, E.L., Schubert, A., Secic, M., Barnett, G., Shutway, F., Ebrahim, Z.Y., 1998. The influence of scalp infiltration with bupivacaine on hemodynamics and postoperative pain in adult patients undergoing craniotomy. Anesthesiol. Analg. 87 (3), 579–582.

Cavallotti, D., Artico, M., De Santis, S., Iannetti, G., Cavallotti, C., 1998. Catecholaminergic innervation of the human dura mater involved in headache. Headache 38 (5), 352–355.

Cicchetti, D.V., 1994. Guidelines, criteria, and rules of thumb for evaluating normed and standardized assessment instruments in psychology. Psychol. Assess. 6 (4), 284.

Engel, J., Jr, Mc.Dermott, Wiebe, M.P., Langfitt, S., Stern, J.T., Dewar, J.M., Kieburtz, K, S., 2012. Early surgical therapy for drug-resistant temporal lobe epilepsy: a randomized trial. JAMA 307 (9), 922–930. https://doi.org/10.1001/jama.2012.220.

Fontaine, D., Almairac, F., 2017. Pain during awake craniotomy for brain tumor resection. Incidence, causes, consequences and management. Neurochirurgica 63 (3), 204–207. https://doi.org/10.1016/j.neuchi.2016.08.005.

Fontaine, D., Almairac, F., Santucci, S., Fernandez, C., Dallel, R., Pallud, J., Lanteri-Minet, M., 2018. Dural and pial pain-sensitive structures in humans: new inputs from awake craniotomies. Brain 141 (4), 1040–1048. https://doi.org/10.1093/brain/awy005.

Gfroerer, S., Metzger, R., Fiegel, H., Ramachandran, P., Rolle, U., 2010. Differential changes in intrinsic innervation and interstitial cells of Cajal in small bowel atresia in newborns. World J. Gastroenterol. 16 (45), 5716–5721. https://doi.org/10.3748/wjg.v16.i45.5716.

Guilfoyle, M.R., Helmy, A., Duane, D., Hutchinson, P.J., 2013. Regional scalp block for postcraniotomy analgesia: a systematic review and meta-analysis. Anesthesiol. Analg. 116 (5), 1093–1102. https://doi.org/10.1213/ANE.0b013e3182863c22.

Headache Classification Committee of the International Headache, S. (2013). The International Classification of Headache Disorders, 3rd edition (beta version). Cephalalgia, 33(9), 629–808. doi:10.1177/0333102413485658.

Ives-Deliperi, V., Butler, J.T., 2017. Quality of life one year after epilepsy surgery. Epilepsy Behav 75, 213–217. https://doi.org/10.1016/j.yebeh.2017.08.014.

Johansson, R.S., Vallbo, A.B., 1979. Tactile sensibility in the human hand: relative and absolute densities of four types of mechanoreceptive units in glabrous skin. J. Physiol. 286, 283–300. https://doi.org/10.1113/jphysiol.1979.sp012619.

Kaur, A., Selwa, L., Fromes, G., Ross, D.A., 2000. Persistent headache after supratentorial craniotomy. Neurosurgery 47 (3), 633–636.

Kemp 3rd, W.J., Tubbs, R.S., Cohen-Gadol, A.A., 2012. The innervation of the cranial dura mater: neurosurgical case correlates and a review of the literature. World Neurosurg. 78 (5), 505–510. https://doi.org/10.1016/j.wneu.2011.10.045.

Lee, S.H., Hwang, S.J., Koh, K.S., Song, W.C., Han, S.D., 2017. Macroscopic innervation of the dura mater covering the middle cranial fossa in humans correlated to neurovascular headache. Front. Neuroanat. 11, 127. https://doi.org/10.3389/fnana.2017.00127.

Lee, S.H., Shin, K.J., Koh, K.S., Song, W.C., 2017. Visualization of the tentorial innervation of human dura mater. J. Anat. 231 (5), 683–689. https://doi.org/10.1111/joa.12659.

Lutman, B., Bloom, J., Nussenblatt, B., Romo, V., 2018. A contemporary perspective on the management of post-craniotomy headache and pain. Curr. Pain Headache Rep. 22 (10), 69. https://doi.org/10.1007/s11916-018-0722-4.

Lv, X., Wu, Z., Li, Y., 2014. Innervation of the cerebral dura mater. Neuroradiol. J. 27 (3), 293–298. https://doi.org/10.15274/NRJ-2014-10052.

Messlinger, K., Hanesch, U., Baumgartel, M., Trost, B., Schmidt, R.F., 1993. Innervation of the dura mater encephali of cat and rat: ultrastructure and calcitonin gene-related peptide-like and substance P-like immunoreactivity. Anat. Embryol. 188 (3), 219–237.

Molnar, L., Simon, E., Nemes, R., Fulesdi, B., Molnar, C., 2014. Postcraniotomy headache. J. Anesth. 28 (1), 102–111. https://doi.org/10.1007/s00540-013-1671-z.

Mouraux, A., Rage, M., Bragard, D., Plaghki, L., 2012. Estimation of intraepidermal fiber density by the detection rate of nociceptive laser stimuli in normal and pathological conditions. Neurophysiol. Clin. 42 (5), 281–291. https://doi.org/10.1016/j.neucli.2012.05.004.

Penfield, W., McNaughton, F., 1940. Dural headache and innervation of the dura mater. Arch. Neurol. & Psychiatry 44 (1), 43–75.

Phillips, K., Clauw, D.J., 2011. Central pain mechanisms in chronic pain states–maybe it is all in their head. Best Pract. Res. Clin. Rheumatol 25 (2), 141–154. https://doi.org/10.1016/j.berh.2011.02.005.

Ray, B.S., Wolff, H.G., 1940. Experimental studies on headache: pain-sensitive structures of the head and their significance in headache. Arch. Surg. 41 (4), 813–856. https://doi.org/10.1001/archsurg.1940.01210040002001.

Rivat, C., Becker, C., Blugeot, A., Zeau, B., Mauborgne, A., Pohl, M., Benoliel, J.J., 2010. Chronic stress induces transient spinal neuroinflammation, triggering sensory hypersensitivity and long-lasting anxiety-induced hyperalgesia. Pain 150 (2), 358–368. https://doi.org/10.1016/j.pain.2010.05.031.

Rocha-Filho, P.A., 2015. Post-craniotomy headache: a clinical view with a focus on the persistent form. Headache 55 (5), 733–738. https://doi.org/10.1111/head.12563.

Rocha-Filho, P.A., Gherpelli, J.L., de Siqueira, J.T., Rabello, G.D., 2008. Post-craniotomy headache: characteristics, behaviour and effect on quality of life in patients operated for treatment of supratentorial intracranial aneurysms. Cephalalgia 28 (1), 41–48. https://doi.org/10.1111/j.1468-2982.2007.01465.x.

Schley, M., Bayram, A., Rukwied, R., Dusch, M., Konrad, C., Benrath, J., Schmelz, M., 2012. Skin innervation at different depths correlates with small fibre function but not with pain in neuropathic pain patients. Eur. J. Pain 16 (10), 1414–1425. https://doi.org/10.1002/j.1532-2149.2012.00157.x.

Schueler, M., Neuhuber, W.L., De Col, R., Messlinger, K., 2014. Innervation of rat and human dura mater and pericranial tissues in the parieto-temporal region by meningeal afferents. Headache 54 (6), 996–1009. https://doi.org/10.1111/head.12371.

Steiger, H.J., Tew Jr., J.M., Keller, J.T., 1982. The sensory representation of the dura mater in the trigeminal ganglion of the cat. Neurosci. Lett. 31 (3), 231–236. https://doi.org/10.1016/0304-3940(82)90025-8.

Strassman, A.M., Weissner, W., Williams, M., Ali, S., Levy, D., 2004. Axon diameters and intradural trajectories of the dural innervation in the rat. J. Comp. Neurol. 473 (3), 364–376. https://doi.org/10.1002/cne.20106.

Wiebe, S., Blume, W.T., Girvin, J.P., Eliasziw, M., 2001. A randomized, controlled trial of surgery for temporal-lobe epilepsy. N. Engl. J. Med. 345 (5), 311–318. https://doi.org/10.1056/NEJM200108023450501.

Zhou, H., Ou, M., Yang, Y., Ruan, Q., Pan, Y., Li, Y., 2016. Effect of skin infiltration with ropivacaine on postoperative pain in patients undergoing craniotomy. SpringerPlus 5 (1), 1180. https://doi.org/10.1186/s40064-016-2856-3.